CONF-9706113--7

PULSE TRANSFORMER R&D FOR NLC KLYSTRON PULSE MODULATOR[*]

M. Akemoto[†], S. Gold, A. Krasnykh and R. Koontz
Stanford Linear Accelerator Center, Stanford University, Stanford CA 94309

DISCLAIMER

Abstract

We have studied a conventional pulse transformer for the NLC klystron pulse modulator. The transformer has been analyzed using a simplified lumped circuit model. It is found that a fast rise time requires low leakage inductance and low distributed capacitance and can be realized by reducing the number of secondary turns, but it produces larger pulse droop and requires a larger core size. After making a tradeoff among these parameters carefully, a conventional pulse transformer with a rise time of 250ns and a pulse droop of 3.6% has been designed and built. The transmission characteristics and pulse time-response were measured. The data were compared with the model. The agreement with the model was good when the measured values were used in the model simulation. The results of the high voltage tests using a klystron load are also presented.

MASTER

PULSE TRANSFORMER R&D FOR NLC KLYSTRON PULSE MODULATOR*

M. Akemoto[†], S. Gold, A. Krasnykh and R. Koontz
Stanford Linear Accelerator Center, Stanford University, Stanford CA 94309

Abstract

We have studied a conventional pulse transformer for the NLC klystron pulse modulator. The transformer has been analyzed using a simplified lumped circuit model. It is found that a fast rise time requires low leakage inductance and low distributed capacitance and can be realized by reducing the number of secondary turns, but it produces larger pulse droop and requires a larger core size. After making a tradeoff among these parameters carefully, a conventional pulse transformer with a rise time of 250ns and a pulse droop of 3.6% has been designed and built. The transmission characteristics and pulse time-response were measured. The data were compared with the model. The agreement with the model was good when the measured values were used in the model simulation. The results of the high voltage tests using a klystron load are also presented.

1. Introduction

The klystron pulse modulator for the Next Linear Collider(NLC) is required to produce a 500kV, 530A pulse width, 1.5µs flat top to drive a pair of PPM-focused 75MW klystron[1]. The R&D of basic elements, a charging supply , a PFN, a thyratron switch tube and a pulse transformer for a prototype NLC modulator is being performed at SLAC[2].

The power efficiency of the modulator is extremely important. The effective output power of the modulator is the power of the flat-top portion of the high voltage output pulse. Since a pulse transformer is a major contributor to the waveform, the pulse transformer requires a fast rise time. In order to achieve a rise time that is less than 400ns, we have improved the design of a 14:1 pulse transformer by tradeoffs among the droop, the core size and the rise time. The test transformer has been built, and low and high voltage tests have been performed.

2. Analysis of the pulse transformer

In this section, we discuss the rise time, core size and pulse droop of a pulse transformer using a lumped circuit model. In order to simplify the analysis, we consider a simple geometrical arrangement with rectangular core. A single-layer secondary is wound over a one-layer primary and the distance between layers is constant[3].

2.1 Equivalent circuit

Figure 1 shows an equivalent circuit for the pulse transformer including an ideal turns ratio of 1:n. The L_P is primary inductance, the L_S is secondary inductance, the L_L is leakage inductance, the C_D is distributed capacitance, the L_D is distributed leakage inductance. We shall neglect core loss and nonlinearity of the core. These circuit elements can be calculated from the geometrical constants of the transformer, the dielectric constant of the insulation, and the permeability of the core material.
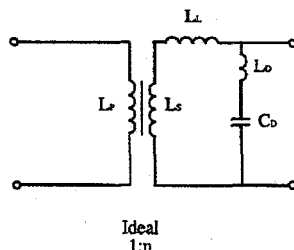

Figure 1. Equivalent circuit for the pulse transformer.

2

DISCLAIMER

Portions of this document may be illegible
in electronic image products. Images are
produced from the best available original
document.

2.2 Droop and core size

The droop D_r is given by

$$D_r = \frac{R_{kly} \cdot \tau}{2L_s} , \qquad (1)$$

where R_{kly} is the klystron impedance, τ the pulse width and L_s the secondary inductance.
The cross-section area of the core A is given by

$$A = \frac{V_s \tau}{\Delta B} \frac{1}{N_s} , \qquad (2)$$

where V_s is the voltage of secondary, N_s the number of secondary turns and ΔB the total magnetic flux density swing of the core. Thus, the cross-sectional area of the core is inversely proportional to the number of secondary turns.
The secondary inductance L_s is calculated by

$$L_s = \frac{\mu_0 \mu_e A \cdot N_s^2}{l} , \qquad (3)$$

where μ_0 is the permeability of free space, μ_e the effective magnetic permeability and l the length of the magnetic path. Thus, the droop D_r is given by

$$D_r = \frac{\Delta B \cdot R_{kly}}{2\mu_0 \mu_e V_s} \frac{l}{N_s} . \qquad (4)$$

The droop is propoportinal to the length of the magnetic path and inversely to proportional to the number of secondary turns. From Equation (2) and (4), the core volume V_{core} is given by

$$V_{core} = Al = \frac{2\mu_0 \mu_e}{\Delta B^2} P \cdot \tau \cdot D_r , \qquad (5)$$

where P is the peak power of the output pulse. Thus, the core volume is independent of the number of turns and proportional to the droop and the output pulse power $(P\tau)$.

2.3 Rise time

The rise time t_r is determined by

$$t_r \propto \sqrt{L_L \cdot C_D} . \qquad (6)$$

The leakage inductance L_L is calculated by

$$L_L \propto \frac{\mu_0 \Delta \cdot u \cdot N_s^2}{L} , \qquad (7)$$

where Δ is the distance between layers, u the average circumference of the layers and L the winding length.
The distributed capacitance C_D is calculated by

$$C_D \propto \frac{\varepsilon_0 \varepsilon_r u \cdot L}{\Delta} \left(\frac{n-1}{n}\right)^2 , \qquad (8)$$

3

where ε_0 is the permittivity of free space, ε_r the dielectric constant of the insulation and n the turns ratio. Therefore, by using $u \approx 4\sqrt{A}$, we find that the rise time is given by

$$t_r \propto \sqrt{\varepsilon_r} \sqrt{\frac{V_s \cdot \tau}{\Delta B}} \sqrt{N_s} \frac{n-1}{n} . \tag{9}$$

It is found that the rise time strongly depends on the number of the secondary turns and is almost independent of the turns ratio.

2.4 Tradeoffs

From the above analysis, it is found that a fast rise time requires low leakage inductance and low distributed capacitance and can be realized by reducing the number of secondary turns, but it produces larger pulse droop and requires a larger core size. Since a droop of several percent can be compensated by making adjustments to the PFN, we can improve the rise time by tradeoffs among the parameters.

3. Fabrication of test pulse transformer

The conventional pulse transformer has been carefully designed and optimized by model calculations. The transformer is an isolation transformer type with two parallel primary basket windings, and with two parallel tapered secondary basket windings as shown in Figure 2. It has been fabricated by Stangenes Industries, Inc. Parallel primaries and secondaries are wound on each leg providing bifilar characteristics. The core is made up of 3 smaller subcores strapped together. Each subcore is wound from 0.002-inches thick, silectron grain-oriented silicon steel ribbon. Table I and II shows specifications and parameters of the pulse transformer, respectively.
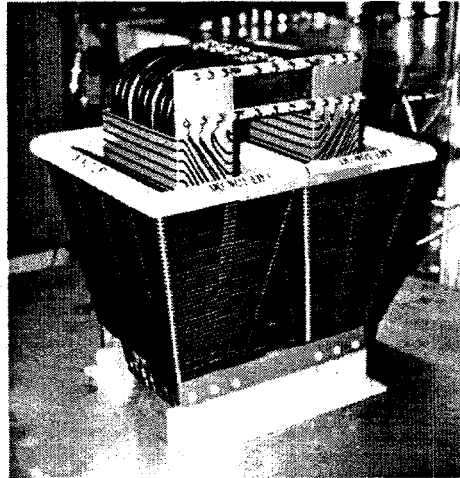

Figure 2. Side view of the pulse transformer.

Table I. Specification of the pulse transformer

Primary voltage	33.2 kV
Primary current	5320 A
Secondary voltage	465 kV
Secondary current	380 A
Output impedance	1224 Ω
Flat top pulse width	1.5 μs
Pulse droop	3.6 %
Rise time	250 ns
Turns ratio	1:14
Pulse repetition rate	180 pps

4

Table II. Parameters of the pulse transformer

Parameters	unit	
Total magnetic flux density swing(ΔB)	T	2.0
Effective magnetic permeability(μ_e)		1,500
Core packing factor(P_f)	%	89
Area of the core(A/P_f)	m^2	0.0102
Distance between layers in the high-voltage side	mm	52
Distance between layers in the low-voltage side	mm	6
Mean magnetic-path length(l)	m	1.04
Effective winding length(L)	mm	260
Circumference of the primary layer	mm	550
Number of primary turns(N_P)	turns	3
Number of secondary turns(N_s)	turns	42

4. Low voltage Tests[4]

The low voltage tests of the pulse transformer were performed in air.

4.1 Equivalent circuit parameters

The primary inductance, secondary inductance, leakage inductance and the distributed capacitance between the primary and the secondary windings were measured with an LCR meter (BK Precision 875A). In the model calculation, the shape of the tapered basket, the distribution of voltage along the windings and the bobbin insulation were considered. The measured and calculated parameters for the pulse transformer are summarized in Table III. The measured and calculated d-c capacitance between the primary and the secondary windings were 210pF and 160pF, respectively. We are investigating the discrepancy between the calculations and the measurements. It should be noted that the calculated value does not include the inductance of the shorting strap across the primary. If the shorting is 200nH, 39.2μH should be subtracted from the measured value and in this case, close agreement between measured and calculated values is obtained.

Table III. Equivalent circuit parameters for the pulse transformer in air

Item	unit	Model calculated value	Measured value
Primary Inductance(L_p)	μH	130	55.2
Secondary Inductance(L_s)	mH	25.48	10.81
Distributed capacitance(C_D)	pF	25	33
Leakage inductance(L_1)	μH	80.4	122.2

4.2 Transmission characteristics

The transmission characteristics of the pulse transformer were measured with the network analyzer(HP 3577A). The test circuit is shown in Figure 3.
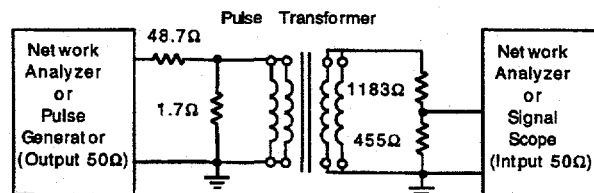

Figure 3. Test circuit.

5

Figure 4 shows the data of the amplitude and phase for the transformer as a function of frequency. A remarkable feature of the measurement data is a prominent sharp dip at 7.198MHz. This frequency corresponds to $1/2\pi\sqrt{L_D C_D}$. Using the measured distributed capacitance, we find that the distributed inductance L_D is 14.8μH. The broken curve in this figure shows result simulated by a computer code Micro-Cap IV using the equivalent circuit parameters of the measured values. The simulation gives a good fit to the data, but in the range of more than 8MHz the model is in disagreement with data.
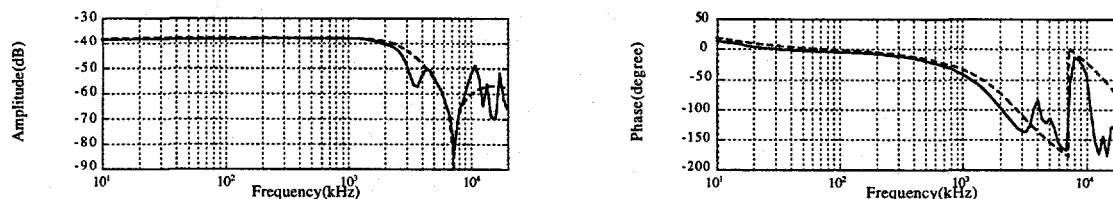

Figure 4. Amplitude and phase for the pulse transformer as a function of frequency.

4.3 Pulse response

A square low-voltage pulse signal with a width of 2μs was fed to the primary side, and the output pulse waveform was measured with the oscilloscope as shown in Figure 3. The result is shown in Figure 5. The rise time(10-90%) was 190ns. Thus, the rise time in oil is estimated to be 280ns and almost satisfies the design value. The broken curve in this figure shows simulated result. The simulation gives a good fit to the data. To fit the overshoot of the waveform, a distributed capacitance of ~50pF is required.
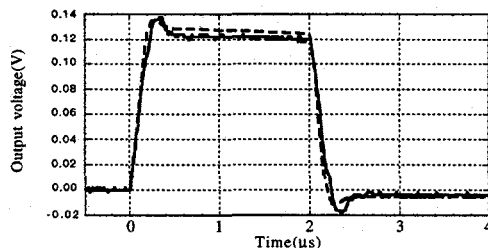

Figure 5. Pulse response of the pulse transformer.

5. High voltage test

The high voltage test of the pulse transformer connected to a 5045 klystron has performed in oil. The transformer was operated by a conventional line type modulator consisting of three parallel PFNs with 11 sections.

5.1 Output pulse waveform

The solid line in Figure 6 shows an example of the klystron voltage waveform. An output pulse with a peak voltage of 405kV and a rise time of 430ns(10-90%) was successfully generated. The PFN was not adjusted to make a flat-top.

5.2 Distributed capacitance

There are distributed capacitances in between the pulse transformer and the oil tank, and the klystron cathode. They have direct effects upon the rise time. We measured the total distributed capacitance experimentally. The klystron voltage and current were measured while switching off the klystron heater. From the relation of the integrated charge and the voltage, the total distributed capacitance was estimated to be ~250pF. The detail of the

6

distributed capacitance is shown in Table IV. The broken curve in Figure 6 shows the result simulated by adding the distributed capacitances into the model circuit. The simulation agrees well with the experimental data. It should be noted that the distributed capacitance for the pulse transformer itself contributes approximately one third to the total distributed capacitance.
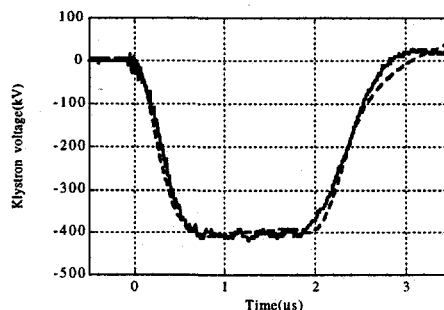

Figure 6. Output pulse waveform at the klystron.

Table IV. Detail of the distributed capacitance

Item	Capacitance(pF)
Klystron cathode	~90
Distributed capacitance for the pulse transformer	~73
Other	~87
Total	~250

6. Summary

For the NLC klystron pulse modulator, we have developed an improved pulse transformer design with a 14 to 1 turns ratio by making tradeoffs among the droop, the core size and the rise time, and have built a test transformer to study its characteristics. In the low voltage test, the transmission characteristics and pulse time-response were measured and the data was compared with the lumped circuit model. The agreement with the model was good when the measured values were used in the model simulation. In the high voltage test of the transformer using a klystron load, an output pulse with a peak voltage of 405kV and a rise time of 430ns was successfully generated.

Acknowledgments

The authors wish to thank George Caryotakis and Ronald Ruth for their support of this project.

References

[1] The NLC Design Group: 'Zeroth-Order Design Report for the Next Linear Collider', SLAC-474, 1996.

[2] R. Koontz, M. Akemoto, S. Gold, A. Krasnykh and Z. Wilson: 'NLC Klystron Pulse Modulator R&D at SLAC', Proc. of the 1997 IEEE Particle Accelerator Conference, 1997.

[3] N. G Glasoe and J.V. Lebacqz: 'Pulse Generators', Massachusetts Institude of Technology Radiation Laboratory Series, vol. 5, McGraw-Hill Book Company, New York, 1948.

[4] M. Akemoto, S. Gold and A. Krasnykh: 'Analysis of the conventional pulse transformer by a lumped circuit model', to be published.